The IEEE 802.15.3a UWB Channel Model as a Two-Dimensional Augmented Cluster Process

John A. Gubner, *Member*, *IEEE*, and Kei Hao

***Abstract*— The IEEE 802.15.3a standards body has developed a modification of the Saleh–Valenzuela (SV) multipath channel model as the accepted channel model for ultra-wideband (UWB) investigations. The SV model is a well-defined simulation model that is straightforward to implement. However, since the model as specified is not directly amenable to theoretical analysis, it is constructed here as a two-dimensional "augmented cluster point process" that is composed of three statistically independent components that can be separately analyzed. For the IEEE 802.15.3a model, general formulas are derived for means, variances, and covariances of important channel quantities. In particular, closed-form expressions in terms of the channel parameters are found in the following cases: the number of multipath arrivals, the number of *detectable* multipath arrivals, the sum of path gains, the sum of squares of path gains, and the received multipath waveform. In addition, closed-form expressions are found for the power-delay profile and the detectable-path profile.**

***Index Terms*— Detectable-path profile, power-delay profile, Saleh–Valenzuela model, shot noise, ultra-wideband.**

I. Introduction

ULTRA-WIDEBAND (UWB) communication systems have recently generated intense interest due to their potential for providing pervasive wireless connectivity [11], [14]. This potential is due to the fact that UWB can provide very high bit rate, low-cost, low-power wireless communication for a wide variety of systems; e.g., personal computer, TV, VCR, CD, DVD, MP3 [2], [11]. Current systems, such as those based on IEEE 802.11b, 11a, or 11g cannot do this because their power consumption and cost are too high [2].

The Federal Communications Commission has allocated 7.5 GHz of spectrum for unlicensed commercial ultra-wideband (UWB) communication systems. In order to develop a common channel model, the IEEE 802.15.3a standards body [6] considered several possibilities and established a modification of the Saleh–Valenzuela (SV) model [12] as the accepted channel model for UWB investigations [2], [9]. The SV model is a well-defined simulation model that is straightforward to implement. Unfortunately, the usual specification of the SV model is not directly amenable to theoretical analysis. To address this difficulty, we develop the SV/IEEE 802.15.3a model as a two-dimensional "augmented cluster point process" that is composed of three statistically independent components that can be separately analyzed. We then exploit this decomposition to derive closed-form expressions for several important quantities, including the power-delay profile and the detectable-path profile.

J. A. Gubner and K. Hao are with the Department of Electrical and Computer Engineering, University of Wisconsin, Madison, WI 53706–1691 USA (e-mail: gubner@engr.wisc.edu, khao@wisc.edu).

Outline of the Paper

Section II introduces the general multipath channel model with enough notation to summarize our results.

In Section III we construct the SV/IEEE 802.15.3a channel model as a two-dimensional augmented cluster process.

Section IV establishes our closed-form results based on more general formulas derived in the Appendixes, and Section V contains the conclusion.

II. Summary of Results

Frequency-selective fading channels are well modeled by time-varying impulse responses of the form [10]

$$h(t,\tau) = \sum_{l=1}^{L(t)} \beta_l(t)\delta(\tau - \tau_l(t)),$$

where t and τ are the observation time and the application time of the impulse, respectively. The total number of multipath components is $L(t)$, the $\{\beta_l(t)\}$ are time-varying gains, and the $\{\tau_l(t)\}$ are the path arrival times or delays. For indoor environments whose structure changes slowly in comparison with the signaling rate, we use the time-invariant model

$$h(\tau) = \sum_{l=1}^{L} \beta_l \delta(\tau - \tau_l).$$

The response of the channel at time t to a transmitted waveform ξ is

$$\rho(t) = \sum_{l=1}^{L} \beta_l \xi(t - \tau_l). \tag{1}$$

Observe that if we put $\varphi(\tau,\beta) := \beta\xi(t-\tau)$, then we can write the response as

$$\sum_{l=1}^{L} \varphi(\tau_l, \beta_l). \tag{2}$$

The sum of a function evaluated at random arguments is called a **shot-noise random variable** [5], [8], [13]. In addition to the channel response, there are many other quantities relevant to the study of wireless channels that can be expressed in terms of shot-noise random variables by the appropriate choice of φ.

1) If $\varphi(\tau,\beta) = I_{[a,b]}(\tau)$, then (2) counts the number of paths arriving in the time window $[a,b]$. Here I is the indicator function: $I_{[a,b]}(\tau) = 1$ if $\tau \in [a,b]$ and is zero otherwise.
2) If $\varphi(\tau,\beta) = I_{[a,b]}(\tau) I_{[1,\infty)}(\beta^2/\beta^2_{\min})$, then (2) counts the number of "detectable" paths that arrive in the time window $[a,b]$. Here "detectable" means that the energy of the path gain is at least $\beta^2_{\min}$.

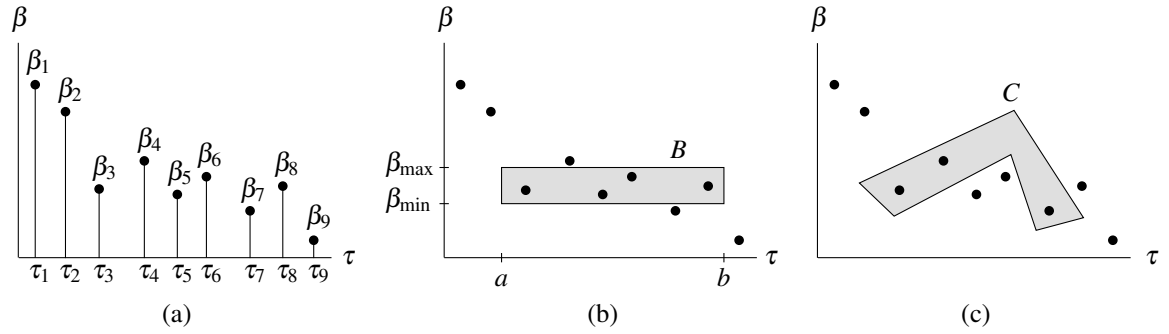

Fig. 1. (a) Graph of delays τ_l and corresponding gains β_l. (b) There are 4 paths that arrive during the time interval $a \le t \le b$ and also have gains lying in the range $\beta_{\min} \le \beta \le \beta_{\max}$. In other words, if $B = [a,b] \times [\beta_{\min}, \beta_{\max}]$ then $N(B) = 4$. (c) The number of delay-gain pairs in the set C is $N(C) = 3$.

3) If $\varphi(\tau,\beta) = \beta I_{[a,b]}(\tau)$, then (2) is equal to the sum of the path gains that arrive in the time window $[a,b]$.
4) If $\varphi(\tau,\beta) = \beta^2 I_{[a,b]}(\tau)$, then (2) is equal to the sum of the squares of the path gains that arrive in the time window $[a,b]$.

In the Appendixes, we derive general formulas for the means, variances, and covariances of shot-noise random variables when the arrival times and gains are distributed according to the IEEE 802.15.3a UWB channel model. In particular, we mention the following special cases studied in the body of the paper.

In Section IV-A, we give closed-form expressions for the mean, variance, and covariance of numbers of paths in nonoverlapping time windows.

Let $\mathscr{D}_\eta(t)$ denote the expected number of paths in $[0,t]$ whose energy is at least a fraction η of the expected energy of the first path. Then the expected number of detectable paths in a small time window $[t, t+\Delta t]$ is

$$\mathscr{D}_\eta(t+\Delta t) - \mathscr{D}_\eta(t) \approx \mathscr{D}'_\eta(t)\Delta t.$$

We call $\mathscr{D}'_\eta(t)$ the **detectable-path profile**. We give closed-form expressions for $\mathscr{D}_\eta(t)$, $\mathscr{D}_\eta(\infty)$, and $\mathscr{D}'_\eta(t)$ in Section IV-B.

In Section IV-C we show that the sum of path gains in a time window has zero mean, and we give a closed-form expression for the variance. We also show that the sums of gains in nonoverlapping time windows are uncorrelated.

Let $\mathscr{E}(t)$ denote the expected sum of squares of channel gains in $[0,t]$. Then the expected sum of squares of gains in a small time window $[t, t+\Delta t]$ is

$$\mathscr{E}(t+\Delta t) - \mathscr{E}(t) \approx \mathscr{E}'(t)\Delta t.$$

Hence, the **power-delay profile** is $\mathscr{E}'(t)/\mathscr{E}(\infty)$. We derive closed-form expressions for $\mathscr{E}(t)$, $\mathscr{E}(\infty)$, and $\mathscr{E}'(t)$ in Section IV-D. In particular, the power-delay profile is shown to consist of two exponentially decaying terms. To estimate the power-delay profile in a real system, we would probe the channel with a short pulse $\xi(t)$ and estimate the second moment of the channel response $\rho(t)$ in (1). We derive simple expressions for $\mathsf{E}[\rho(t)^2]$ in Section IV-E. These formulas show that $\mathsf{E}[\rho(t)^2]$ consists of two exponentially decaying terms of the same rates as the power-delay profile, but with weights that depend in a computable way on the transmitted pulse.

III. The SV/IEEE 802.15.3a Channel Model

Most prior work, e.g., [3], [4], [7], [12], [15], has regarded the delays τ_l as a temporal point process and the β_l as marks as shown in Fig. 1(a). However, we have found it more convenient to regard the pairs (τ_l, β_l) as random points in two-dimensional space as shown in Figs. 1(b) and 1(c) (which contain the same points as Fig. 1(a)). In the general theory of point processes, one focuses on the random *number* of points in different subsets rather than on the random *locations* of the points. For example, if B is the rectangular product set $B = [a,b] \times [\beta_{\min}, \beta_{\max}]$ shown in Fig. 1(b), then the number of points in B, denoted by $N(B)$, is 4. In the context of the multipath channel, $N([a,b] \times [\beta_{\min}, \beta_{\max}])$ is the number of paths that arrive in the time interval $a \le t \le b$ and whose corresponding gains satisfy $\beta_{\min} \le \beta \le \beta_{\max}$. We can also count the number of points that lie in nonrectangular sets. For example, if C is the polygonal set in Fig. 1(c), the number of points in C is $N(C) = 3$.

In the general theory of point process, the quantity $N(B)$ is regarded as a counting measure on the measurable sets B. Hence, instead of (2), one writes the **counting integral**

$$\int\int \varphi(\tau,\beta) N(d\tau \times d\beta).$$

It remains to specify the distribution of the times τ_l and the gains β_l. For example, Turin *et al.* [15] considered modeling the τ_l as the arrival times of a homogeneous Poisson process. Unfortunately, this model was not consistent with the clustering of paths observed in their data [12]. Other researchers have considered inhomogeneous Poisson arrivals [3] and doubly-stochastic Poisson arrivals [4]. However, no one has taken the SV/IEEE 802.15.3a model, which includes the clustering effect, and expressed it as an augmented cluster process in two-dimensional space as we do next. Although the model is *not* a Poisson process, it is built up from Poisson processes, and we exploit this fact to derive analytical formulas that can be evaluated without resorting to simulation.

A. Initial Paths of the Clusters

The ith cluster starts with the path that arrives at time S_{i0}, $i = 0, 1, 2, \ldots$ (see Fig. 2), where the initial cluster always starts at the deterministic time $S_{00} \equiv 0$. The remaining cluster start times, S_{i0}, $i = 1, 2, \ldots$, are taken to be the occurrence times

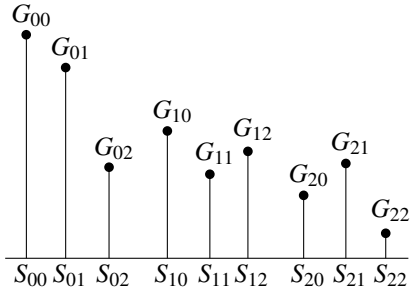

Fig. 2. Multipath arrival times and gains.

of a homogeneous Poisson process of constant intensity C called the **cluster arrival rate**. Given the cluster start times S_{i0}, the corresponding gains G_{i0} are taken to be conditionally independent with each G_{i0} depending only on the value of S_{i0}. Given that $S_{i0} = \tau$, the conditional density of G_{i0} is denoted by $f_{\tau,\tau}(\cdot)$. For $i \geq 1$, the gains G_{i0} can be considered marks of the Poisson cluster start times S_{i0}. Such a marked Poisson process is equivalent to a two-dimensional Poisson process with intensity function [8, Sec. 5.2]

$$\lambda_1(\tau,\gamma) := C f_{\tau,\tau}(\gamma), \quad \tau \geq 0, \gamma \in \mathbb{R}. \tag{3}$$

For future reference, on functions $\varphi(\tau,\gamma)$, we define the linear functional

$$\bar{\Lambda}_1 \varphi = \int_0^\infty \int_{-\infty}^\infty \varphi(\tau,\gamma)\lambda_1(\tau,\gamma)\, d\gamma d\tau. \tag{4}$$

We denote by N_1 the Poisson process with intensity function λ_1. Then the point process consisting of the initial paths of all the clusters is

$$N_c(B) := I_B(S_{00}, G_{00}) + N_1(B). \tag{5}$$

In the construction of cluster processes, N_c is called the cluster **center process** [5].

B. Noninitial Paths of the Clusters

Conditional on the cluster start times $\{S_{i0}, i \geq 0\}$, the arrival times of the noninitial paths in different clusters are modeled as independent homogeneous Poisson processes. Each of these Poisson processes has the same constant intensity R called the **ray arrival rate**. If the initial path of the ith cluster arrives at time $S_{i0} = \tau$ with gain $G_{i0} = \gamma$, and the jth noninitial path of the ith cluster arrives at time $S_{ij} = s$ $(j \geq 1)$, then the gain of this noninitial path, denoted by G_{ij}, has conditional density $f_{\tau,s}(\cdot)$. These gains are conditionally independent and can be considered marks of the Poisson arrival times of the noninitial paths in the cluster. As mentioned above, such a marked Poisson process is equivalent to a two-dimensional Poisson process. Here the intensity function is[1]

$$\lambda_r(s,g|\tau,\gamma) := R f_{\tau,s}(g) I_{[\tau,\infty)}(s). \tag{6}$$

[1]Since the intensity in (6) is zero for $s < \tau$, the Poisson process starts at time τ. This is in contrast to [2] and [12]. Their ray processes were defined by taking Poisson processes starting at time zero and then translating them by the arrival time of the initial path in the cluster. The two constructions are equivalent provided we adjust the definition of $f_{\tau,s}(\cdot)$. This is done in (10) where we use $s-\tau$; [2] and [12] would use only s.

Note that $\lambda_r(s,g|\tau,\gamma)$ depends on τ but not γ. Let

$$\{N_r(\cdot|\tau,\gamma), \tau \geq 0, \gamma \in \mathbb{R}\}$$

denote a family of independent Poisson processes with corresponding intensity functions $\lambda_r(\cdot,\cdot|\tau,\gamma)$. Since the intensity functions do not depend on γ, neither do the processes $N_r(\cdot|\tau,\gamma)$. The process consisting of the noninitial paths of all the clusters is given by

$$N_*(B) := \int_0^\infty \int_{-\infty}^\infty N_r(B|\tau,\gamma)\, N_c(d\tau \times d\gamma).$$

Since N_* results from the placing of independent point process at each point of N_c, N_* is called an **independent cluster process** [5]. In our case, due to the form of N_c in (5), it is advantageous to write

$$N_*(B) = N_r(B|S_{00}, G_{00}) + N_\times(B), \tag{7}$$

where

$$N_\times(B) := \int_0^\infty \int_{-\infty}^\infty N_r(B|\tau,\gamma)\, N_1(d\tau \times d\gamma).$$

First, recalling that $S_{00} \equiv 0$ and that $N_r(\cdot|\tau,\gamma)$ does not depend on γ, we see that

$$N_{r0}(B) := N_r(B|S_{00}, G_{00}) \tag{8}$$

is a Poisson process with intensity $R f_{0,s}(s,g) I_{[0,\infty)}(s)$. Second, conditioned on the points of N_1, $N_\times$ is a sum of independent Poisson processes and is therefore a Poisson process with conditional intensity[2]

$$\int_0^\infty \int_{-\infty}^\infty \lambda_r(s,g|\tau,\gamma)\, N_1(d\tau \times d\gamma).$$

For future reference, we define the linear operator $\bar{\Lambda}_r$ on functions $\varphi(s,g)$ by

$$\begin{aligned}(\bar{\Lambda}_r \varphi)(\tau,\gamma) &:= \int_0^\infty \int_{-\infty}^\infty \varphi(s,g)\lambda_r(s,g|\tau,\gamma)\, dg\, ds \\ &= R\int_\tau^\infty \int_{-\infty}^\infty \varphi(s,g) f_{\tau,s}(g)\, dg\, ds. \end{aligned} \tag{9}$$

Since this does not depend on γ, we sometimes write $(\bar{\Lambda}_r\varphi)(\tau)$ to denote (9).

C. Assumptions about the Densities of the Gains

Following Saleh and Valenzuela [12, eq. (26)] and Batra *et al.* [2, p. 2126], we assume $f_{\tau,s}(\cdot)$ has second moment

$$\Omega_0 e^{-\tau/\tau_0} e^{-(s-\tau)/s_0}, \tag{10}$$

where Ω_0 is a scale factor, and τ_0 and s_0 are **power-delay time constants**. In [12], $f_{\tau,s}(\cdot)$ is taken to be a Rayleigh density. For the IEEE 802.15.3a model in [2], a $\{\pm 1\}$-valued-Bernoulli$(1/2)$ mixture of lognormal densities is used. This implies that under the model in [2], $f_{\tau,s}(\cdot)$ is even and therefore has zero mean. It also implies that if G has density $f_{\tau,s}$, then $10\log_{10} G^2$ is normal with mean

$$\mu_{\tau,s} := \frac{10}{\ln 10}\left[\ln\Omega_0 - \tau/\tau_0 - (s-\tau)/s_0 - \left(\frac{\ln 10}{10}\right)^2 \frac{\sigma^2}{2}\right] \tag{11}$$

and variance σ^2.

[2]Thus, $N_\times$ is a both a cluster process and a doubly-stochastic Poisson process.

D. The SV/IEEE 802.15.3a Point Process

The natural way to define the SV/IEEE 802.15.3a UWB point process N is to write it as the sum of the initial paths plus the noninitial paths; i.e.,

$$N(B) := N_c(B) + N_*(B).$$

Since N results from adding the center process N_c to the cluster process N_*, we call N an **augmented cluster process**.

For analysis purposes, it is advantageous to use (5), (7), and (8) to write

$$N(B) = I_B(S_{00}, G_{00}) + N_1(B) + N_{r0}(B) + N_\times(B).$$

Remark: The above decomposition can be regarded as the sum of the two augmented cluster process

$$I_B(S_{00}, G_{00}) + N_{r0}(B) \quad \text{and} \quad N_1(B) + N_\times(B).$$

The first process always has exactly one center located at the point (S_{00}, G_{00}); note that the first component of the point is deterministic since $S_{00} \equiv 0$. In the second process, the centers are Poisson distributed.

If we put

$$N_\otimes(B) := N_1(B) + N_\times(B), \tag{12}$$

then

$$N(B) = I_B(S_{00}, G_{00}) + N_{r0}(B) + N_\otimes(B),$$

where the three terms on the right are independent. It then follows that any counting integral with respect to the UWB channel process such as

$$\Phi := \int_0^\infty \int_{-\infty}^\infty \varphi(s,g)\, N(ds \times dg) \tag{13}$$

can be expressed as the sum of the three independent terms

$$\Phi = \varphi(0, G_{00}) + \Phi_{r0} + \Phi_\otimes, \tag{14}$$

where

$$\Phi_{r0} := \int_0^\infty \int_{-\infty}^\infty \varphi(s,g)\, N_{r0}(ds \times dg) \tag{15}$$

and

$$\Phi_\otimes := \int_0^\infty \int_{-\infty}^\infty \varphi(s,g)\, N_\otimes(ds \times dg). \tag{16}$$

Line-of-Sight vs. Non-Line-of-Sight Models: The model we have described above in which the initial path arrives at time zero is a line-of-sight (LOS) model. In a non-line-of-sight (NLOS) model, the initial cluster is omitted. For NLOS models, $N(B) = N_\otimes(B)$ and $\Phi = \Phi_\otimes$. All of the formulas below are for LOS models. However, in the figures below pertaining to the channel models CM1–CM4, only CM1 is LOS; CM2–CM4 are NLOS, and in computing the curves in these figures, the unnecessary LOS terms were omitted.

IV. Some Statistics of the IEEE 802.15.3a Model

A. Mean and Covariance of Number of Paths

Let $0 \le a < b \le c < d$, and put $\varphi(s,g) = I_{[a,b]}(s)$ and $\psi(s,g) = I_{[c,d]}(s)$. Let Φ be as in (13) and let Ψ be defined similarly. Then Φ is the number of multipath arrivals in the time window $[a,b]$, and Ψ is the number of multipath arrivals in the time window $[c,d]$. Using (28), (29), and (31) in Appendix C and the simplifications discussed there, it can be shown that

$$\mathsf{E}[\Phi] = I_{[a,b]}(0) + R(b-a) + C(b-a)\left[1 + R\frac{b+a}{2}\right].$$

Since the terms in (14) are independent, with the first being deterministic, $\mathsf{var}(\Phi) = \mathsf{var}(\Phi_{r0}) + \mathsf{var}(\Phi_\otimes)$, and (30) and (33) can be used to show that

$$\mathsf{var}(\Phi) = R(b-a) + C(b-a) \cdot \left[1 + R\frac{3b-a}{2} + R^2(b-a)\left(\frac{b+2a}{3}\right)\right].$$

Similarly,

$$\mathsf{cov}(\Phi, \Psi) = \mathsf{cov}(\Phi_{r0}, \Psi_{r0}) + \mathsf{cov}(\Phi_\otimes, \Psi_\otimes).$$

The first term on the right is zero by the paragraph containing (30). As for $\mathsf{cov}(\Phi_\otimes, \Psi_\otimes)$, which is given by (32), it is argued at the end of Appendix C that the first, second, and fourth terms of (32) are zero. Evaluating the remaining terms, it can be shown that

$$\mathsf{cov}(\Phi, \Psi) = CR(b-a)(d-c)[1 + R(b+a)/2].$$

We make the following observations about the above formula for $\mathsf{E}[\Phi]$. First, the mean number of paths in $[0,t]$ is

$$1 + Rt + Ct(1 + Rt/2), \tag{17}$$

which grows quadratically in t. Second, the expected number of paths in a window $[t, t+\Delta t]$ is

$$I_{[t,t+\Delta t]}(0) + R\Delta t + C\Delta t[1 + R(t + \Delta t/2)],$$

which grows linearly in the position t of the window.

B. Mean Number of Detectable Paths

Recall that the gain of a path arriving at time s as a part of a cluster starting at time τ has second moment given by (10). In particular, the gain of the initial path of the initial cluster arriving at time zero has second moment Ω_0. If we take $\varphi(s,g) = I_{[0,t]}(s) I_{[\eta\Omega_0,\infty)}(g^2)$, then Φ in (13) counts the number of paths arriving in $[0,t]$ that have energy greater than a fraction η of Ω_0. From (28), (29), and (31) in Appendix C,

$$\begin{aligned}\mathscr{D}_\eta(t) := \mathsf{E}[\Phi] &= \mathsf{P}_{0,0}(G^2 \ge \eta\Omega_0) \\ &\quad + R\int_0^t \mathsf{P}_{0,s}(G^2 \ge \eta\Omega_0)\, ds \\ &\quad + C\int_0^t \mathsf{P}_{\tau,\tau}(G^2 \ge \eta\Omega_0)\, d\tau \\ &\quad + CR\int_0^t \int_\tau^t \mathsf{P}_{\tau,s}(G^2 \ge \eta\Omega_0)\, ds\, d\tau,\end{aligned}$$

where $\mathsf{P}_{\tau,s}$ indicates that G is generic random variable with density $f_{\tau,s}(\cdot)$. Since $10\log_{10} G^2$ is normal with mean $\mu_{\tau,s}$ in

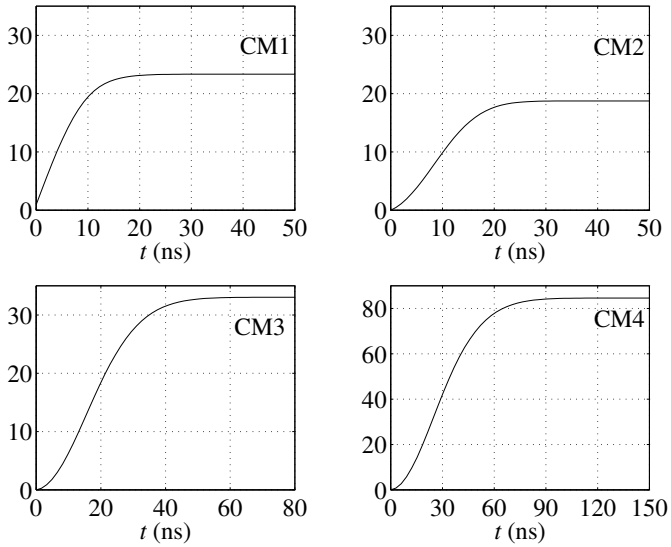

Fig. 3. Mean number of *detectable* paths in $[0,t]$, $\mathscr{D}_\eta(t)$, for $\eta = 0.1$ and channel-model parameters in [2, Table II].

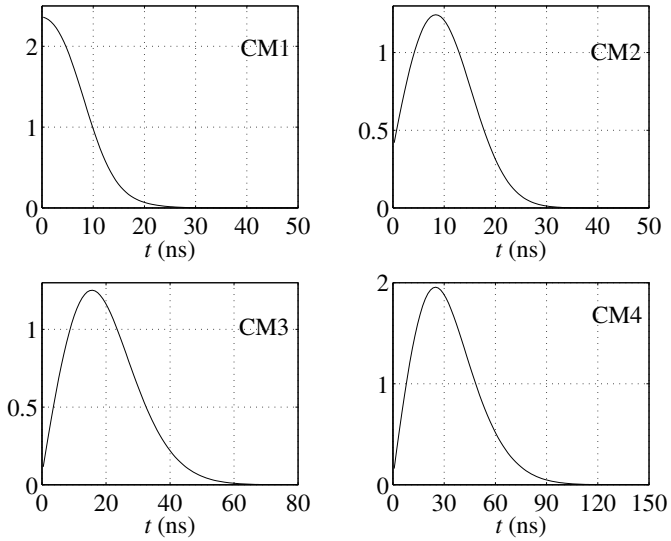

Fig. 4. Detectable-path profiles $\mathscr{D}'_\eta(t)$ corresponding to Fig. 3.

(11) and variance σ^2, we can express $\mathscr{D}_\eta(t)$ in closed form in terms of the standard normal complementary cumulative distribution function $Q(x) := (2\pi)^{-1}\int_x^\infty e^{-t^2/2}\,dt$ using the easily-verified identities

$$H(x) := \int_x^\infty Q(\theta)\,d\theta = \frac{e^{-x^2/2}}{\sqrt{2\pi}} - xQ(x),$$

and

$$J(x) := \int_x^\infty H(t)\,dt = \tfrac{1}{2}[Q(x) - xH(x)].$$

For use later, note that as $x \to \infty$, $Q(x)$, $xH(x)$, and $J(x)$ all tend to zero. A straightforward but tedious calculation shows that with

$$\sigma_* := \sigma\frac{\ln 10}{10} \quad \text{and} \quad \eta_* := \ln\eta + \sigma_*^2/2,$$

we can write

$$\begin{aligned}\mathscr{D}_\eta(t) = {} & Q\big(\tfrac{\eta_*}{\sigma_*}\big) + Rs_0\sigma_*\Big[H\big(\tfrac{\eta_*}{\sigma_*}\big) - H\big(\tfrac{\eta_*+t/s_0}{\sigma_*}\big)\Big] \\ & + C\tau_0\sigma_*\Big[H\big(\tfrac{\eta_*}{\sigma_*}\big) - H\big(\tfrac{\eta_*+t/\tau_0}{\sigma_*}\big)\Big] \\ & + CRs_0\tau_0\sigma_*^2\Big[J\big(\tfrac{\eta_*}{\sigma_*}\big) - \big\{1 - \tfrac{s_0}{s_0-\tau_0}\big\} \\ & \cdot J\big(\tfrac{\eta_*+t/\tau_0}{\sigma_*}\big) - \tfrac{s_0}{s_0-\tau_0}J\big(\tfrac{\eta_*+t/s_0}{\sigma_*}\big)\Big].\end{aligned}$$

We also have

$$\begin{aligned}\lim_{t\to\infty}\mathscr{D}_\eta(t) = {} & Q\big(\tfrac{\eta_*}{\sigma_*}\big) + Rs_0\sigma_*H\big(\tfrac{\eta_*}{\sigma_*}\big) + C\tau_0\sigma_*H\big(\tfrac{\eta_*}{\sigma_*}\big) \\ & + CRs_0\tau_0\sigma_*^2J\big(\tfrac{\eta_*}{\sigma_*}\big).\end{aligned}$$

Graphs of $\mathscr{D}_\eta(t)$ are shown in Fig. 3. Notice that expected number of detectable paths in $[0,t]$ levels off as intuition would suggest. This is in stark contrast to the quadratic growth of the expected total number of paths in (17).

Starting from either the integral formula or the closed-form expression for $\mathscr{D}_\eta(t)$, we can differentiate and obtain the mean detectable-path profile

$$\begin{aligned}\mathscr{D}'_\eta(t) = {} & RQ\big(\tfrac{\eta_*+t/s_0}{\sigma_*}\big) + CQ\big(\tfrac{\eta_*+t/\tau_0}{\sigma_*}\big) \\ & + CR\tfrac{s_0\tau_0}{s_0-\tau_0}\sigma_*\Big[H\big(\tfrac{\eta_*-t/s_0}{\sigma_*}\big) - H\big(\tfrac{\eta_*-t/\tau_0}{\sigma_*}\big)\Big].\end{aligned}$$

Graphs of $\mathscr{D}'_\eta(t)$ are shown in Fig. 4.

C. Mean and Covariance of Sum of Path Gains in a Time Window

Let $0 \le a < b \le c < d$ as above, and put $\varphi(s,g) = gI_{[a,b]}(s)$ and $\psi(s,g) = gI_{[c,d]}(s)$. Then Φ in (13) is the sum of the gains of the multipath arrivals in the time window $[a,b]$, and Ψ, defined similarly to Φ, is the sum of the gains of the multipath arrivals in the time window $[c,d]$. Using (28), (29), and (31) along with the fact that $f_{\tau,s}(\cdot)$ has zero mean, it is easy to show that $\mathsf{E}[\Phi] = 0$. Using (30), and again using the fact that $(\bar{\Lambda}_r\varphi)(\tau) = 0$ in (33), we find that

$$\begin{aligned}\mathsf{var}(\Phi) = {} & I_{[a,b]}(0)E[G_{00}^2] + R\int_a^b \mathsf{E}_{0,s}[G^2]\,ds \\ & + \bar{\Lambda}_1(\varphi^2) + \bar{\Lambda}_1(\bar{\Lambda}_r(\varphi^2)),\end{aligned} \tag{18}$$

where G is a generic random variable with density $f_{0,s}(\cdot)$. On account of (10), (18) is computable in closed form. For example, the integral term is

$$\Omega_0 Rs_0(e^{-a/s_0} - e^{-b/s_0}),$$

and

$$\bar{\Lambda}_1(\varphi^2) = \Omega_0 C\tau_0(e^{-a/\tau_0} - e^{-b/\tau_0}).$$

A bit more work shows that the last term in (18) can also be expressed in closed form. It is

$$\begin{aligned}\bar{\Lambda}_1(\bar{\Lambda}_r(\varphi^2)) = {} & \Omega_0 CR\big[\zeta(a,b,s_0)\zeta\big(0,a,s_0\tau_0/(s_0-\tau_0)\big) \\ & + s_0\zeta(a,b,\tau_0) \\ & - s_0\zeta\big(a,b,s_0\tau_0/(s_0-\tau_0)\big)e^{-b/s_0}\big],\end{aligned}$$

where

$$\zeta(a,b,\mu) := \mu[e^{-a/\mu} - e^{-b/\mu}].$$

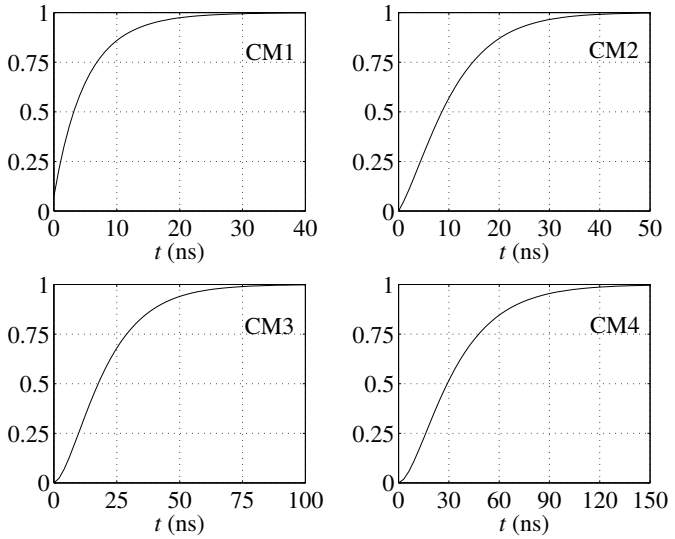

Fig. 5. Normalized mean sum of squares of path gains arriving in $[0,t]$, $\mathscr{E}(t)/\mathscr{E}(\infty)$, for channel-model parameters in [2, Table II].

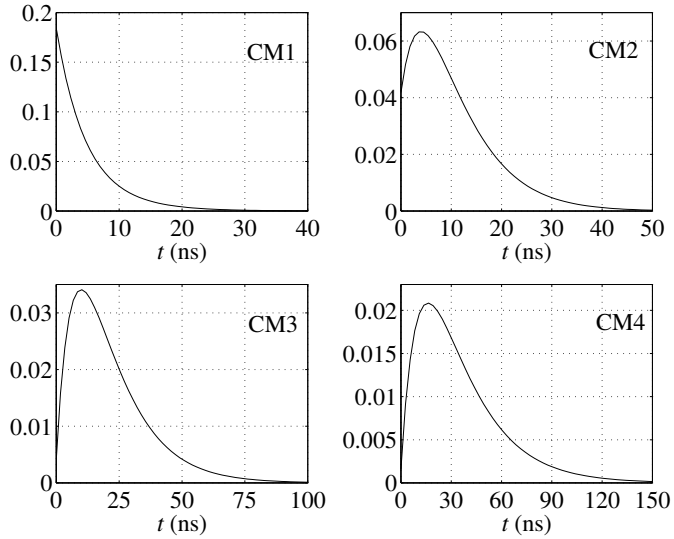

Fig. 6. Power-delay profiles $\mathscr{E}'(t)/\mathscr{E}(\infty)$ for channel-model parameters in [2, Table II].

If we put $a=0$ and let $b\to\infty$, we find that

$$\lim_{b\to\infty}\mathsf{var}(\Phi)=\Omega_0[1+Rs_0+C\tau_0+CRs_0\tau_0]. \tag{19}$$

We conclude this subsection by writing

$$\mathsf{cov}(\Phi,\Psi)=\mathsf{cov}(\varphi(0,G_{00}),\psi(0,G_{00}))+\mathsf{cov}(\Phi_{r0},\Psi_{r0})+\mathsf{cov}(\Phi_{\otimes},\Psi_{\otimes}).$$

The first term on the right is zero since the intervals $[a,b]$ and $[c,d]$ are disjoint. The second term is zero by the paragraph containing (30). As for $\mathsf{cov}(\Phi_{\otimes},\Psi_{\otimes})$, it is argued at the end of Appendix C that the first, second, and fourth terms of (32) are zero. However, the remaining terms involve $\bar{\Lambda}_r\psi$, which is zero since $\mathsf{E}_{\tau,s}[G]=0$. Thus,

$$\mathsf{cov}(\Phi,\Psi)=0,$$

and we see that the sums of gains in different time windows are uncorrelated.

D. Expected Sum of Squares of Path Gains

If we are interested in the sum of the *squares of* the gains in an interval, we can take $\widetilde{\varphi}(s,g)=g^2I_{[a,b]}(s)$ and define $\widetilde{\Phi}$ similarly to (13). If we then use the formulas of Appendix C to compute $\mathsf{E}[\widetilde{\Phi}]$, we get exactly (18). This is easy to see as follows. Let $\varphi(s,g)=gI_{[a,b]}(s)$ as in the preceding subsection. Then observe that since the square of an indicator is equal to itself, $\widetilde{\varphi}(s,g)=g^2I_{[a,b]}(s)=\varphi(s,g)^2$; e.g., $\bar{\Lambda}_1(\varphi^2)=\bar{\Lambda}_1\widetilde{\varphi}$.

It now follows that by taking $a=0$ and $b=t$ in (18), we obtain the expected channel power in $[0,t]$, which we denoted earlier by $\mathscr{E}(t)$. Appealing to the formulas between (18) and (19) inclusive, and putting $\zeta_\mu(t):=\mu[1-e^{-t/\mu}]$, we find that

$$\mathscr{E}(t)=\Omega_0\Big\{1+R\zeta_{s_0}(t)+C\zeta_{\tau_0}(t)+RCs_0\Big[\zeta_{\tau_0}(t)-\zeta_{s_0\tau_0/(s_0-\tau_0)}(t)e^{-t/s_0}\Big]\Big\},$$

and

$$\mathscr{E}(\infty)=\Omega_0[1+Rs_0+C\tau_0+CRs_0\tau_0].$$

Fig. 5 shows graphs of $\mathscr{E}(t)/\mathscr{E}(\infty)$.

From the formula for $\mathscr{E}(t)$, it immediately follows that

$$\mathscr{E}'(t)=\Omega_0\Big\{R[1+Cs_0\tau_0/(s_0-\tau_0)]e^{-t/s_0}+C[1-Rs_0\tau_0/(s_0-\tau_0)]e^{-t/\tau_0}\Big\},\quad t>0, \tag{20}$$

and the power-delay profile $\mathscr{E}'(t)/\mathscr{E}(\infty)$ is easily computed. Graphs are shown in Fig. 6.

With (20) it would be easy to use the MATLAB function `fzero` to find the delay t at which the power-delay profile decays to, say -60 dB. However, we have by inspection that for large t, the decay is dominated by the slower-decaying of the two terms in (20). If $s_0>\tau_0$, the decay will be according to e^{-t/s_0}; otherwise the decay will be according to e^{-t/τ_0}. For example, if $\tau_0>s_0$, the approximation

$$10\log_{10}\Big[\Omega_0C[1-Rs_0\tau_0/(s_0-\tau_0)]e^{-t/\tau_0}/\mathscr{E}(\infty)\Big]\approx -60$$

is linear in t and can be trivially solved. An analogous linear equation holds if $s_0>\tau_0$. For the channel parameters in [2, Table II], the approximate solution agrees with the exact solution using `fzero` in at least the first two digits.

E. Mean and Covariance of the UWB Channel Response

If we take $\varphi(s,g)=g\xi(t_1-s)$ and $\psi(s,g)=g\xi(t_2-s)$, and if Ψ is defined similarly to Φ in (13), then $\Phi=\rho(t_1)$ and $\Psi=\rho(t_2)$, where $\rho(t)$ is the UWB waveform seen at the receiver. Using the formulas in Appendix C, it is not hard to show that $\mathsf{E}[\rho(t_1)]=0$, and

$$\begin{aligned}\mathsf{cov}(\rho(t_1),\rho(t_2))&=\mathsf{E}[G_{00}^2]\xi(t_1)\xi(t_2)\\&\quad+R\int_0^\infty\xi(t_1-s)\xi(t_2-s)\mathsf{E}_{0,s}[G^2]\,ds\\&\quad+C\int_0^\infty\xi(t_1-\tau)\xi(t_2-\tau)\mathsf{E}_{\tau,\tau}[G^2]\,d\tau\\&\quad+CR\int_0^\infty\int_\tau^\infty\xi(t_1-s)\xi(t_2-s)\mathsf{E}_{\tau,s}[G^2]\,ds\,d\tau.\end{aligned}$$

Note that this last double integral can be reduced to a single integral by changing the order of integration and using (10). In particular, it is straightforward to verify that

$$\mathsf{E}[\rho(t)^2] = \Omega_0\Big\{\xi(t)^2 + R\Xi_{s_0}(t) + C\Xi_{\tau_0}(t) + \frac{s_0\tau_0}{s_0-\tau_0}CR\big[\Xi_{s_0}(t)-\Xi_{\tau_0}(t)\big]\Big\}, \qquad (21)$$

where

$$\Xi_\mu(t) := \int_0^\infty \xi(t-\theta)^2 e^{-\theta/\mu}\,d\theta.$$

Furthermore, since $\int_{-\infty}^{\infty}\Xi_\mu(t)\,dt = \mu\|\xi\|^2$, where $\|\xi\|^2 := \int_{-\infty}^{\infty}\xi(t)^2\,dt$ is the energy in the waveform ξ, it follows easily that the expected total energy in the received waveform ρ is

$$\mathsf{E}\left[\int_{-\infty}^{\infty}\rho(t)^2\,dt\right] = \int_{-\infty}^{\infty}\mathsf{E}[\rho(t)^2]\,dt = \|\xi\|^2\Omega_0\big\{1+Rs_0+C\tau_0+CRs_0\tau_0\big\}.$$

Notice that this is proportional to $\mathscr{E}(\infty)$.

We make the following observations about $\Xi_\mu(t)$. First, it is the unilateral Laplace transform of $\xi(t-\cdot)^2$ evaluated at $1/\mu$. Second, if ξ is a suitably normalized short-duration pulse, then we can approximate $\xi(t-\theta)^2$ by the unit impulse $\delta(t-\theta)$ and see that $\Xi_\mu(t) \approx e^{-t/\mu}$. Substituting this into (21) yields, for $t>0$, $\mathsf{E}[\rho(t)^2] \approx \mathscr{E}'(t)$. As we noted below (20), for large t, $\mathscr{E}'(t)$ decays exponentially fast at a rate determined by the larger of s_0 and τ_0. In fact, when ξ is any finite-duration pulse, the same is true of $\mathsf{E}[\rho(t)^2]$ even without the impulse approximation. Suppose that ξ is causal and of duration T. Then for $t>T$,

$$\Xi_\mu(t) = e^{-t/\mu}\underbrace{\int_0^T \xi(\tau)^2 e^{\tau/\mu}\,d\tau}_{=:\xi_\mu},$$

and we can write

$$\mathsf{E}[\rho(t)^2] = \Omega_0\Big\{R[1+Cs_0\tau_0/(s_0-\tau_0)]\xi_{s_0}e^{-t/s_0} + C[1-Rs_0\tau_0/(s_0-\tau_0)]\xi_{\tau_0}e^{-t/\tau_0}\Big\},$$

which differs from (20) only by the weights ξ_{s_0} and ξ_{τ_0}; the exponential decay rates are not affected. This shows in terms of the channel parameters the simple relationship between the power-delay profile that would be determined by probing the channel with a real pulse ξ and the exact profile obtained with an ideal impulse.

V. Conclusion

We have presented a careful development of the SV/IEEE 802.15.3a UWB channel model as an augmented cluster point process that is composed of three statistically independent components that can be separately analyzed. We have shown that important channel quantities can be expressed as shot-noise random variables driven by the augmented cluster process, and we have derived formulas for means, variances, and covariances of such shot-noise random variables. In particular, we have derived closed-form expressions for the detectable-path profile, the power-delay profile, and other important channel statistics.

Appendix A
Poisson-Driven Shot-Noise Random Variables

Let $N_1(\cdot)$ be a Poisson process on a space $\boldsymbol{X}$ [8, Ch. 2].[3] In other words, for $A \subset \boldsymbol{X}$, $N_1(A)$ denotes the number of points in A. The random variable $N_1(A)$ is Poisson, and we denote its mean value by

$$\Lambda_1(A) := \mathsf{E}[N_1(A)].$$

When $N_1(A)$ is regarded as a function of A, $N_1(\cdot)$ is a nonnegative, integer-valued measure. When $\Lambda_1(\cdot)$ is regarded as a function of A, we call $\Lambda_1(\cdot)$ the **mean measure** of $N_1(\cdot)$.

If v is a function on $\boldsymbol{X}$, we define the shot-noise random variable [8, Ch. 3]

$$V := \int v(x)\,N_1(dx). \qquad (22)$$

Then

$$\mathsf{E}[V] = \int v(x)\,\Lambda_1(dx),$$

where we assume $v \in L^1(\Lambda_1)$ both here and in (22) in order that the integrals be well defined. If we also have $w \in L^1(\Lambda_1)$ and define

$$W := \int w(x)\,N_1(dx),$$

then

$$\mathsf{E}[VW] = \int v(x)w(x)\,\Lambda_1(dx) + \left[\int v(x)\,\Lambda_1(dx)\right]\left[\int w(x)\,\Lambda_1(dx)\right],$$

where we additionally assume $v, w \in L^2(\Lambda_1)$. We also have the moment generating function

$$\mathsf{E}[e^{sV}] = \exp\left[\int [e^{sv(x)}-1]\,\Lambda_1(dx)\right],$$

where s is complex and $[e^{sv(\cdot)}-1] \in L^1(\Lambda_1)$.

In order to write the preceding expectations in a more compact form, we define the linear functional

$$\bar{\Lambda}_1 v := \int v(x)\Lambda_1(dx) \qquad (23)$$

so that

$$\mathsf{E}[V] = \bar{\Lambda}_1 v, \quad \mathsf{E}[VW] = \bar{\Lambda}_1(v\cdot w) + \bar{\Lambda}_1 v\cdot\bar{\Lambda}_1 w,$$

and

$$\mathsf{E}[e^{sV}] = \exp\big[\bar{\Lambda}_1\big(e^{sv(\cdot)}-1\big)\big].$$

Appendix B
Analysis of Integrals with Respect to $N_1(\cdot)$ and $N_\times(\cdot)$

Doubly-Poisson Cluster Processes

Let $N_1(\cdot)$ be the Poisson process defined in Appendix A with mean measure $\Lambda_1(\cdot)$ and the linear functional $\bar{\Lambda}_1$ defined in (23). Let $\{N_r(\cdot|x), x \in \boldsymbol{X}\}$ be a family of independent Poisson

[3] For the purposes of this paper, $\boldsymbol{X} = [0,\infty)\times\mathbb{R}$, but we state the results in Appendix A for an arbitrary space $\boldsymbol{X}$.

processes on a set $\boldsymbol{Y}$.[4] Assume the $N_r(\cdot|x)$ are independent of $N_1(\cdot)$. Denote the mean measure of $N_r(\cdot|x)$ by $\Lambda_r(\cdot|x)$.

We now define the cluster process $N_\times(\cdot)$ on $\boldsymbol{Y}$ by [5, Ch. 8]

$$N_\times(B) := \int N_r(B|x)\,N_1(dx), \quad B \subset \boldsymbol{Y}.$$

Because $N_1(\cdot)$ is a Poisson process, $N_\times(\cdot)$ is called a **Poisson cluster process** [5]. Since $N_r(\cdot|x)$ is also Poisson, we call $N_\times(\cdot)$ a **doubly-Poisson cluster process**. If we let $\mathscr{N}_1$ denote the σ-field generated by $N_1(\cdot)$, then conditioned on $\mathscr{N}_1$, $N_\times(\cdot)$ is a sum of independent Poisson processes. Hence, conditioned on $\mathscr{N}_1$, the mean measure of $N_\times(\cdot)$ is

$$M_\times(B) := \mathsf{E}[N_\times(B)|\mathscr{N}_1] = \int \Lambda_r(B|x)\,N_1(dx).$$

In other words, because the $N_r(\cdot|x)$ are independent Poisson processes that are independent of $N_1(\cdot)$, $N_\times(\cdot)$ is a doubly-stochastic Poisson process with conditional mean measure $M_\times(\cdot)$. Thus, $N_\times(\cdot)$ is both a cluster process and a doubly-stochastic Poisson process.

Doubly-Poisson-Cluster-Driven Shot-Noise Random Variables

Let p and q be functions defined on $\boldsymbol{Y}$, and introduce the cluster-process-driven shot-noise random variables

$$P := \int p(y)\,N_\times(dy) \quad \text{and} \quad Q := \int q(y)\,N_\times(dy).$$

Then

$$\mathsf{E}[P|\mathscr{N}_1] = \int p(y)\,M_\times(dy) = \int \left[\int p(y)\,\Lambda_r(dy|x)\right] N_1(dx).$$

It is now convenient to introduce the operator notation

$$(\bar{\Lambda}_r p)(x) := \int p(y)\,\Lambda_r(dy|x)$$

so that we can write

$$\mathsf{E}[P|\mathscr{N}_1] = \int p(y)\,M_\times(dy) = \int (\bar{\Lambda}_r p)(x)\,N_1(dx), \tag{24}$$

which we recognize as a Poisson-driven shot-noise random variable analogous to (22). A similar argument shows that

$$\begin{aligned}\mathsf{E}[PQ|\mathscr{N}_1] &= \int p(y)q(y)\,M_\times(dy) \\ &\quad + \left[\int p(y)\,M_\times(dy)\right]\left[\int q(y)\,M_\times(dy)\right] \\ &= \int (\bar{\Lambda}_r p \cdot q)(x)\,N_1(dx) \\ &\quad + \left[\int (\bar{\Lambda}_r p)(x)\,N_1(dx)\right]\left[\int (\bar{\Lambda}_r q)(x)\,N_1(dx)\right].\end{aligned} \tag{25}$$

Since the integrals in (24) and (25) are Poisson-driven shot-noise random variables, taking expectations yields

$$\mathsf{E}[P] = \bar{\Lambda}_1(\bar{\Lambda}_r p)$$

and

$$\begin{aligned}\mathsf{E}[PQ] = \bar{\Lambda}_1(\bar{\Lambda}_r(p\cdot q)) + \bar{\Lambda}_1((\bar{\Lambda}_r p)\cdot(\bar{\Lambda}_r q)) \\ + \bar{\Lambda}_1(\bar{\Lambda}_r p)\cdot\bar{\Lambda}_1(\bar{\Lambda}_r q).\end{aligned}$$

[4]For the purposes of this paper, $\boldsymbol{Y} = \boldsymbol{X} = [0,\infty)\times\mathbb{R}$, but we state the results in Appendix B for an arbitrary spaces $\boldsymbol{X}$ and $\boldsymbol{Y}$.

We also need that

$$\begin{aligned}\mathsf{E}[VP|\mathscr{N}_1] &= V\mathsf{E}[P|\mathscr{N}_1] \\ &= V\int (\bar{\Lambda}_r p)(x)\,N_1(dx),\end{aligned}$$

which is a product of Poisson-driven shot-noise random variables. Hence,

$$\mathsf{E}[VP] = \bar{\Lambda}_1(v\cdot(\bar{\Lambda}_r p)) + \bar{\Lambda}_1(v)\cdot\bar{\Lambda}_1(\bar{\Lambda}_r p).$$

Example: Using the foregoing formulas, it is easy to see that

$$\mathsf{E}[V+P] = \bar{\Lambda}_1(v) + \bar{\Lambda}_1(\bar{\Lambda}_r p), \tag{26}$$

and

$$\begin{aligned}\mathsf{cov}(V+P, W+Q) &= \bar{\Lambda}_1(v\cdot w) + \bar{\Lambda}_1(w\cdot\bar{\Lambda}_r p) \\ &\quad + \bar{\Lambda}_1(v\cdot\bar{\Lambda}_r q) + \bar{\Lambda}_1(\bar{\Lambda}_r(p\cdot q)) \\ &\quad + \bar{\Lambda}_1((\bar{\Lambda}_r p)\cdot(\bar{\Lambda}_r q)).\end{aligned} \tag{27}$$

APPENDIX C
ANALYSIS OF SV/IEEE 802.15.3A COUNTING INTEGRALS

As shown in Section III-D, under the SV/IEEE 802.15.3a model, a counting integral of the form Φ in (13) can be written as the sum of the three statistically independent terms in (14). We now derive general formulas for some statistics of these terms. Motivated by the specific counting integrals in Section IV, we restrict attention to integrands $\varphi(s,g)$ of product form, say $\varphi_1(s)\varphi_2(g)$.

The First Component

When $\varphi(s,g) = \varphi_1(s)\varphi_2(g)$,

$$\mathsf{E}[\varphi(0, G_{00})] = \varphi_1(0)\mathsf{E}[\varphi_2(G_{00})]. \tag{28}$$

If $\varphi(s) = I_{[a,b]}(s)$ and $a > 0$, then $\varphi_1(0) = 0$. If $\varphi_2(g)$ is equal to g or g^2 and $f_{0,0}$ is Rayleigh or the IEEE 802.15.3a lognormal mixture, $\mathsf{E}[\varphi_2(G_{00})]$ is available in closed form.

The Second Component

We next consider Φ_{r0} in (15). As noted following (8), N_{r0} is a Poisson process with intensity $Rf_{0,s}(s,g)I_{[0,\infty)}(s)$. Hence, by the results in Appendix A,

$$\mathsf{E}[\Phi_{r0}] = (\bar{\Lambda}_r\varphi)(0),$$

where $\bar{\Lambda}_r$ was defined in (9). If φ has product form, we can write

$$\mathsf{E}[\Phi_{r0}] = (\bar{\Lambda}_r\varphi)(0) = R\int_0^\infty \varphi_1(s)\mathsf{E}_{0,s}[\varphi_2(G)]\,ds, \tag{29}$$

where G is a generic random variable with density $f_{0,s}(\cdot)$. For φ_2 a polynomial, the expectation will typically be available in closed form, usually as an exponential in s (cf. (10)); if we also have $\varphi_1(s) = I_{[a,b]}(s)$, then $(\bar{\Lambda}_r\varphi)(0)$ can be computed in closed form.

Analogous to (15), suppose we have another integral Ψ_{r0} of a function $\psi(s,g)$ also of product form. Then the covariance between these two Poisson-driven counting integrals is

$$\begin{aligned}\mathsf{cov}(\Phi_{r0}, \Psi_{r0}) &= (\bar{\Lambda}_r(\varphi\cdot\psi))(0) \\ &= R\int_0^\infty \varphi_1(s)\psi_1(s)\mathsf{E}_{0,s}[\varphi_2(G)\psi_2(G)]\,ds.\end{aligned}$$

If φ_1 and ψ_1 are indicator functions of disjoint intervals, then the covariance is zero. If the intervals are the same, say $[a,b]$, then

$$\mathsf{cov}(\Phi_{r0},\Psi_{r0}) = R\int_a^b \mathsf{E}_{0,s}[\varphi_2(G)\psi_2(G)]\,ds. \tag{30}$$

As noted above, there are interesting cases in which this expectation and integral will be computable in closed form.

The Third Component

We now focus on the properties of $\Phi_\otimes$ in (16). On account of (12), we can write $\Phi_\otimes = V + P$, where

$$V := \int_0^\infty \int_{-\infty}^\infty \varphi(\tau,\gamma) N_1(d\tau \times d\gamma)$$

and

$$P := \int_0^\infty \int_{-\infty}^\infty \varphi(s,g) N_\times(ds \times dg).$$

Since $\mathsf{E}[V+P]$ is given by (26) in Appendix B, we have

$$\mathsf{E}[\Phi_\otimes] = \bar{\Lambda}_1(\varphi) + \bar{\Lambda}_1(\bar{\Lambda}_r\varphi), \tag{31}$$

where $\bar{\Lambda}_1$ is the linear functional defined in (4) and $\bar{\Lambda}_r$ is the linear operator defined in (9).

Now suppose that $\Psi_\otimes$ is defined similarly to $\Phi_\otimes$. Then we can similarly write $\Psi_\otimes = W + Q$ and see that

$$\mathsf{cov}(\Phi_\otimes,\Psi_\otimes) = \mathsf{cov}(V+P, W+Q)$$

which is given by (27) in Appendix B. Thus,

$$\begin{aligned}\mathsf{cov}(\Phi_\otimes,\Psi_\otimes) = {} & \bar{\Lambda}_1(\varphi\cdot\psi) + \bar{\Lambda}_1(\psi\cdot\bar{\Lambda}_r\varphi) + \bar{\Lambda}_1(\varphi\cdot\bar{\Lambda}_r\psi) \\ & + \bar{\Lambda}_1(\bar{\Lambda}_r(\varphi\cdot\psi)) + \bar{\Lambda}_1((\bar{\Lambda}_r\varphi)\cdot(\bar{\Lambda}_r\psi)).\end{aligned} \tag{32}$$

We also record the special case,

$$\begin{aligned}\mathsf{var}(\Phi_\otimes) = {} & \bar{\Lambda}_1(\varphi^2) + 2\bar{\Lambda}_1(\varphi\cdot\bar{\Lambda}_r\varphi) \\ & + \bar{\Lambda}_1(\bar{\Lambda}_r(\varphi^2)) + \bar{\Lambda}_1((\bar{\Lambda}_r\varphi)^2).\end{aligned} \tag{33}$$

Simplifications of (31)–(33): The assumptions of the IEEE 802.15.3a model allow for several further simplifications in the formulas for $\bar{\Lambda}_1$ and $\bar{\Lambda}_r$. This makes the computation of (31)–(33) quite tractable.

We first consider $\bar{\Lambda}_r$. Since $\lambda_r(s,g|\tau,\gamma)$ is defined in (6) not to depend on γ, we write

$$(\bar{\Lambda}_r\varphi)(\tau) = \int_0^\infty \int_{-\infty}^\infty \varphi(s,g)\lambda_r(s,g|\tau,\gamma)\,ds\,dg.$$

Next, since we will be concerned only with functions φ of product form, e.g., $\varphi(s,g) = \varphi_1(s)\varphi_2(g)$, we can further exploit the definition of λ_r to write

$$(\bar{\Lambda}_r\varphi)(\tau) = R\int_\tau^\infty \varphi_1(s)\mathsf{E}_{\tau,s}[\varphi_2(G)]\,ds,$$

where G is a generic random variable with density $f_{\tau,s}$ mentioned in (6). Note that if $\varphi_1(s) = I_{[a,b]}(s)$ for some $0 \le a < b$, then $(\bar{\Lambda}_r\varphi)(\tau) = 0$ for $\tau > b$. Also, since G has an even density, if φ_2 is odd, $(\bar{\Lambda}_r\varphi)(\tau) = 0$.

We next consider $\bar{\Lambda}_1$. If ψ also has product form, and if we exploit the definition of λ_1 in (3), then

$$\bar{\Lambda}_1(\varphi\cdot\psi) = C\int_0^\infty \varphi_1(\tau)\psi_1(\tau)\mathsf{E}_{\tau,\tau}[\varphi_2(\Gamma)\psi_2(\Gamma)]\,d\tau,$$

where Γ is a generic random variable with density $f_{\tau,\tau}$ mentioned in (3). Note that if $0 \le a < b \le c < d$, and $\varphi_1(s) = I_{[a,b]}(s)$ and $\psi_1(s) = I_{[c,d]}(s)$, then $\varphi\cdot\psi = 0$ and the first and fourth terms in (32) are zero.

We can now write

$$\bar{\Lambda}_1(\psi\cdot\bar{\Lambda}_r\varphi) = C\int_0^\infty \psi_1(\tau)(\bar{\Lambda}_r\varphi)(\tau)\mathsf{E}_{\tau,\tau}[\psi_2(\Gamma)]\,d\tau.$$

Note that if φ_1 and ψ_1 are indicators of disjoint intervals as above, then the second term in (32) is zero. Also, since Γ has an even density, if ψ_2 is odd, $\bar{\Lambda}_1(\psi\cdot\bar{\Lambda}_r\varphi) = 0$.

For the calculations we consider here, the expectations $E_{\tau,\tau}$ and $E_{\tau,s}$ will always be available in closed form. Hence, the first term in (31) and in (32) involve at most one integral. The second term in (31) and the second through fourth terms in (32) require at most a double integral. The last term in (32) may require a triple integral, unless $\varphi_2 = \psi_2$, in which case at most a double integral is necessary. In some cases, all terms can be computed in closed form.

REFERENCES

[1] M. Abramowitz and I. A. Stegun, eds. *Handbook of Mathematical Functions, with Formulas, Graphs, and Mathematical Tables*. New York: Dover, 1970.

[2] A. Batra, J. Balakrishnan, G. R. Aiello, J. R. Foerster, and A. Dabak, "Design of a multiband OFDM system for realistic UWB channel environments," *IEEE Trans. Microwave Theory Tech.*, vol. 52, no. 9, pp. 2123–2138, Sept. 2004.

[3] C. D. Charalambous, N. Menemenlis, O. H. Kabranov, and D. Makrakis, "Statistical analysis of multipath fading channels using shot-noise analysis: An introduction," *Proc. IEEE Int. Conf. Commun.*, vol. 4, pp. 1011–1015, June 2001.

[4] C. D. Charalambous and N. Menemenlis, "Statistical analysis of the received signal over multipath fading channels via generalization of shot-noise," *Proc. IEEE Int. Conf. Commun.*, vol. 7, pp. 2246–2250, June 2001.

[5] D. J. Daley and D. Vere-Jones, *An Introduction to the Theory of Point Processes*. New York: Springer, 1988.

[6] J. Foerster, Ed., "Channel Modeling Sub-committee Report Final," IEEE, Document IEEE P802.15-02/490r1-SG3a, 2003.

[7] R. J. Fontana, "An insight into UWB interference from a shot noise perspective," *Proc. IEEE Conf. Ultra Wideband Systems and Technologies*, pp. 309–313, May 2002.

[8] J. F. C. Kingman, *Poisson Processes*. Oxford, U.K.: Clarendon, 1993.

[9] A. F. Molisch, J. R. Foerster, and M. Pendergrass, "Channel models for ultrawideband personal area networks," *IEEE Wireless Communications*, vol. 10, no. 6, pp. 14–21, Dec. 2003.

[10] J. G. Proakis, *Digital Communications*, 4th ed. Boston: McGraw-Hill, 2001.

[11] S. Roy, J. R. Foerster, V. S. Somayazulu, and D. G. Leeper, "Ultra-wideband radio design: The promise of high-speed, short-range wireless connectivity," *Proc. IEEE*, vol. 92, no. 2, pp. 295–311, Feb. 2004.

[12] A. A. M. Saleh and R. Valenzuela, "A statistical model for indoor multipath propagation," *IEEE J. Select. Areas Commun.*, vol. SAC-5, no. 2, pp. 128–137, Feb. 1987.

[13] D. L. Snyder and M. I. Miller, *Random Point Processes in Time and Space*, 2nd ed. New York: Springer, 1991.

[14] S. Stroh, "Ultra wideband: Multimedia unplugged," *IEEE Spectrum*, vol. 40, no. 9, pp. 23–27, Sept. 2004.

[15] G. L. Turin, F. D. Clapp, T. L. Johnston, S. B. Fine, and D. Lavry, "A statistical model of urban multipath propagation," *IEEE Trans. Veh. Technol.*, vol. VT-21, pp. 1–9, Feb. 1972.